The antimatter component induced by cosmic rays in the atmosphere

Taoufik Djemil[*], Réda Attallah[*] and Jean-Noël Capdevielle[†]

[*]*Laboratoire de Physique des Rayonnement (LPR), Université Badji Mokhtar, Annaba, Algérie.*
[†]*AstroParticules et Cosmologie (APC), Université Paris 7, Paris, France.*

Abstract. **After comparing the energy spectrum of nucleon-antinucleon at very high altitude with the Bess experiment, we have simulated the fluxes of antiprotons and antineutrons generated at various atmospheric depths. The simulations are carried out with the help of CORSIKA program involving a primary energy spectrum starting above the energy threshold of antiparticle production up to 1 PeV. Different abundances of alpha and heavy primaries in the primary composition are combined. Specific effects are investigated when the energy of the antiparticles is close to the maximum of the annihilation cross section in antiproton-air interaction. Typical signatures are expected in detectors at atmospheric depths of 100-300 g/cm^2.**

Keywords**: atmospheric antimatter, antiprotons, antineutrons.**

I. Introduction

Atmospheric antiprotons and antineutrons are produced when primary cosmic rays of high energy enter the Earth's atmosphere and interact with air nuclei. They carry important information about the physical processes of their production and propagation in the atmosphere. They are also important for understanding the energy spectrum of galactic antinucleons since their production and propagation mechanisms should be similar. Besides, atmospheric antiprotons represent a significant background for the galactic antiprotons measured by balloon-borne experiments and thus have to be estimated with a good accuracy by model calculations.

There have been several measurements of the atmospheric antiprotons. We have used here the atmospheric antiproton flux measurements of the BESS-2001 experiment [1] which was carried out in September 2001 at Ft. Summer (USA). It is a recent and very precise balloon-borne experiment consisting of a high resolution spectrometer with a large acceptance, capable of performing precise measurements of absolute fluxes of various cosmic rays and their dependence on the atmospheric depth. The vertical geomagnetic cut-off throughout the BESS-2001 flight was about 4.2 GV. The atmospheric antiproton spectrum was measured in the kinetic energy range 0.2-3.4 GeV at an atmospheric depth lying from 4.5 to 26 g/cm^2 (average $\backsimeq$10 g/cm^2) during the slow descending period of the balloon flight.

With the help of CORSIKA code version 6.617 [2], we have performed a set of Monte Carlo calculations concerning the atmospheric antinucleons created by primary cosmic rays. We have calculated the atmospheric antiproton and antineutron energy spectra, then their longitudinal developement in the range 5-300 g/cm^2 and their lateral distribution. We have used for this purpose SIBYLL model version 2.1 [3] for the hadronic interaction above 80 GeV/nucleon and FLUKA model version 2008.3.7 [4] at lower energy. The high energy model plays here a secondary role because of the relatively high altitude (5-300 g/cm^2) of the simulations and the relatively low antinucleon kinetic energy (0.2-10.6 GeV) taken into account. In contrast, the low energy hadronic model is of crucial importance for these altitudes and energies.

The atmospheric density variation is described by the US standard atmosphere [5]. In spite of being an average annual model, this model is suitable for the season of the BESS-2001 experiment because of the high altitudes of observations (24.5-37 km). Unlike low altitudes (0-25 km) where measured atmospheric profiles differ significantly from the US model because of seasonal variations, at higher altitude the difference is not significant (less than a few g/cm^2) [6].

II. Atmospheric antinucleon spectra

The calculation of the atmospheric antiproton and antineutron flux with CORSIKA starts by selecting the type of the primary particle, its energy range, and the altitude of the observation levels. The zenith angle of the primary particle varies randomly from 0 to 70°. The different primary particles, i.e. protons and α-particles, are simulated in separate runs. The energy of the primary cosmic ray particle varies between the energy threshold of antiparticle production up to 1 PeV, according to a power law with a spectral index equal to 2.732 for protons and 2.699 for α-particle [7]. In order to cover all the primary energy spectrum appropriately, a run is carried out for each energy decade separately. The number of events per run varies from 5×10^6 at the lowest energies to 1.4×10^4 at the highest energies. The primary particle is tracked up to the first interaction point determined from the cross section of its interaction with air. The nuclear reaction is then handled by the selected hadronic interaction model, namely FLUKA below 80 GeV/nucleon and SYBILL above 80 GeV/nucleon.

All the secondary particles are tracked up to their decay or further interactions. The zenith angle θ of reg-

istered antiprotons and antineutrons was limited within $\cos\theta \geq 0.84$ [8]. For simplicity, we have omitted in this study to work out statistical errors. Nevertheless, we have used for each run a large number of trials (between 1.4×10^4 and 5×10^6 depending on primary energy and primary particle) to ensure that statistical errors are as small as possible in a reasonable computing time. The antiproton and antineutron fluxes have been calculated for different momentum bins and different atmospheric depths between 5 to 300 g/cm^2.

The results of our Monte Carlo calculations are compared in Fig. 1, on the one hand, to the experimental data of BESS-2001 [1] and, on the other hand, to the calculations of Stephens [9] which are based on the transport equations. In Fig. 1a, the differential energetic spectra of the atmospheric antiprotons is shown for different atmospheric depth lying from 5 to 300 g/cm^2. In Fig. 1b the growth curves are plotted for differents kinetic energy bins. The agreement with experimental data is fairly good except for kinetic energies below 1 GeV. It should be noticed that at these low energies, the experimental cross section for antiproton production is not well known. Fig. 1 also shows that the maximum of the antimatter flux is obtained for an energy of about 1 GeV and at a depth of about 100 g/cm^2.

III. Longitudinal distributions

We have treated characteristic cases of extensive air shower evolution due to primary proton, α-particle and iron. For all these cases, we assume a vertical incidence of the cosmic ray particle, with a fixed energies equal to 10 TeV and 100 TeV. The Linsley standard atmospheric model is used. The longitudinal developments of atmospheric antiprotons and antineutrons are plotted in Fig. 2. As shown, an increase in the number of atmospheric antinucleons occurs in the first 200 g/cm^2, after which there is a continuous decrease due to different interaction processes. The maximum of atmospheric antinucleons is reached for a depth lying in the range 100-300 g/cm^2, of course the higher the energy the deeper the maximum. These results corroborate our calculation of the antinucleon fluxes in the previous section.

IV. Lateral distributions

As known, air showers are not only one-dimensional phenomenon. Because secondary cosmic rays receive transverse momenta as a result of coulomb scattering, they are widely distributed in a three-dimensionel cascade. Fig. 3 shows the lateral distribution in air, parametrised by the US standard model, for atmospheric antiprotons and antineutrons with kinetic energy $E_{kin} \geq 1\ GeV$ at an altitude of 200 g/cm^2. The primary cosmic ray particle is chosen in turn as a proton, an α-particle and finally an iron nucleus. The primary energy is fixed to 10 TeV and 100 TeV. We have focused our attention on the shower core where most secondary cosmic ray hadrons are found. At low energy (10 TeV), light cosmic rays (proton and α-particle) produce about five times more antinucleons near the shower axis than heavy nuclei (iron). However, at higer energy (100 TeV), the contribution from different primaries are quiet similar near the shower axis, with a clear predominance of heavy cosmic ray nuclei just several meters far from the shower axis. These features can be used for the discremination between light and heavy primary nuclei in cosmic ray experiments.

V. Conclusion

The atmospheric antiproton and antineutron low energy spectra are calculated for atmospheric depth lying from 5 to 300 g/cm^2 using the CORSIKA package in a three-dimensional Monte Carlo simulation. The hadronic interaction is treated by the SYBILL model above 80 GeV/nucleon and FLUKA model below this value. The primary cosmic ray spectra of protons and α-particles, the only primary particles considered here, are taken according to a power law. The parametrization of the US standard atmosphere is used to describe the atmospheric density profile. Our numerical results match well with the atmospheric antiproton spectra measured by the BESS-2001 experiment in the kinetic energy range 1-3 GeV. However, below 1 GeV, there is a disagreement which might be due to the poor knowledge of the antiproton production cross section at these low energies. On the other hand, at higher energy, the Monte Carlo results are lower than those obtained with the transport equation calculations. This deviation could be explained by the lack of contribution of the heavy primary cosmic ray particles which might be added. The longitudinal distributions of antiprotons and antineutrons with $E_{kin} \geq 1$ GeV have been simulated for primary particle energies equal to 10 TeV and 100 TeV. The atmospheric antinucleon lateral distributions at 200 g/cm^2 are also obtained.

References

[1] K. Yamato *et al.* , Physics Letters B **632** (2006) 475.
[2] D. Heck *et al.* , Report FZKA 6019 (1998) Forschugszentrum Karlsruhe.
[3] R. Engel *et al.* , Proc. 26th ICRC, 1 (1999) 415.
[4] A. Fassó *et al.* , INFN/TC-05/11, SLAC-R-773, CERN 2005-10 (2005).
A. Fassó et al., CHEP 2003, La Jolla, CA, USA (2003).
[5] J. Linsley, private communication by M Hillas (1988).
[6] B. Wilczyńska *et al.* , Proc. 28th Int. Cosmic Ray Conf.(Tsukuba) 2 (2003) 571.
[7] S. Haino *et al.* , Phys. Lett. B **594** (2004) 35.
[8] T. Sanuki *et al.* , Phys. Lett. B **577** (2003) 10.
[9] S. A. Stephens, Astropart. Phys. **6** (1997) 229.

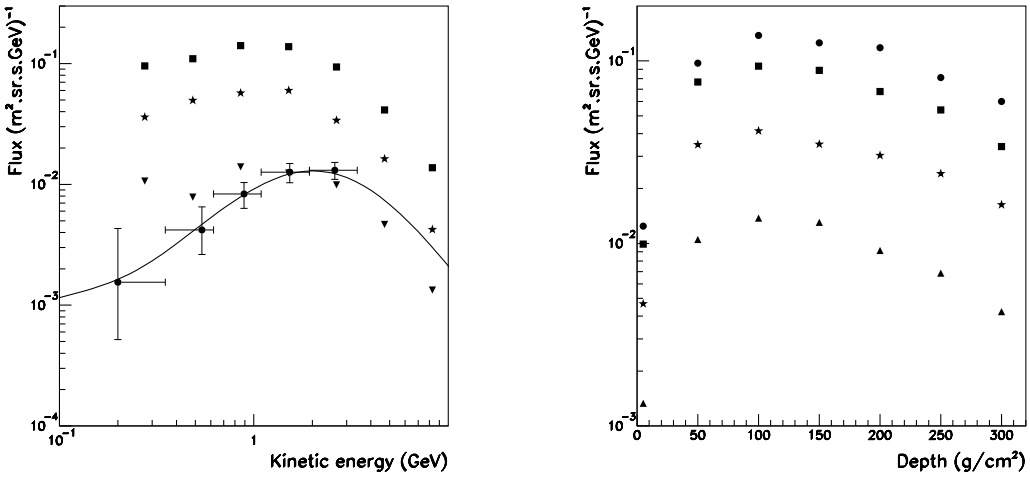

(a) (b)

Fig. 1. Monte Carlo calculations of the atmospheric antiproton energy spectrum. (a) The differential energetic spectra of antiprotons at 5 g/cm^2 (▾), 100 g/cm^2 (■) and 300 g/cm^2 (⋆) compared to experimental data of BESS-2001 (●) [1] and to the transport equation calculations (solid line) [9]. (b) The antiprotons growth curves for kinetic energy equal to 1.51 GeV (●), 2.665 GeV (■), 4.7 GeV (⋆) and 8.28 GeV (▲).

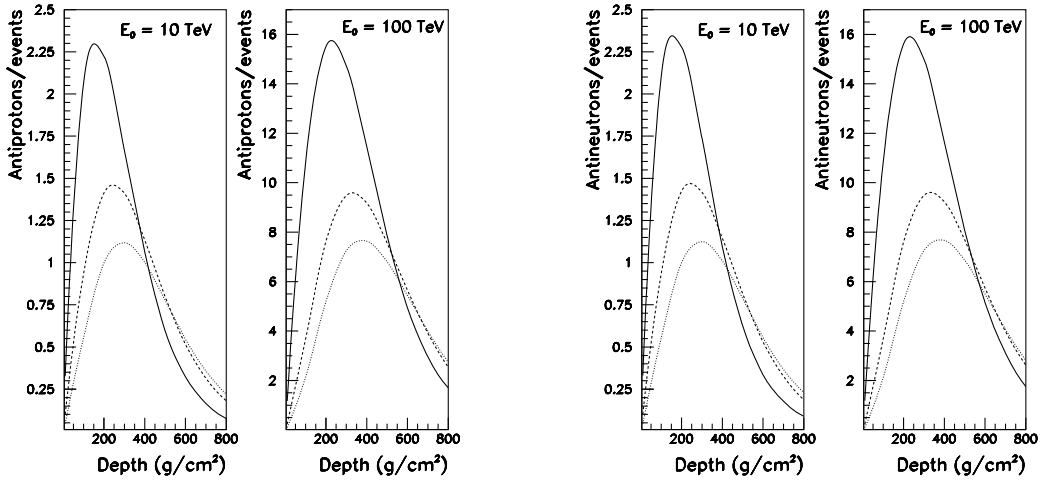

(a) (b)

Fig. 2. Longitudinal distribution of (a) antiprotons and (b) antineutrons with $E_{kin} \geq 1$ GeV produced by vertical primary iron (solid line), α-particle (dashed line) and proton (dotted line) with fixed energy.

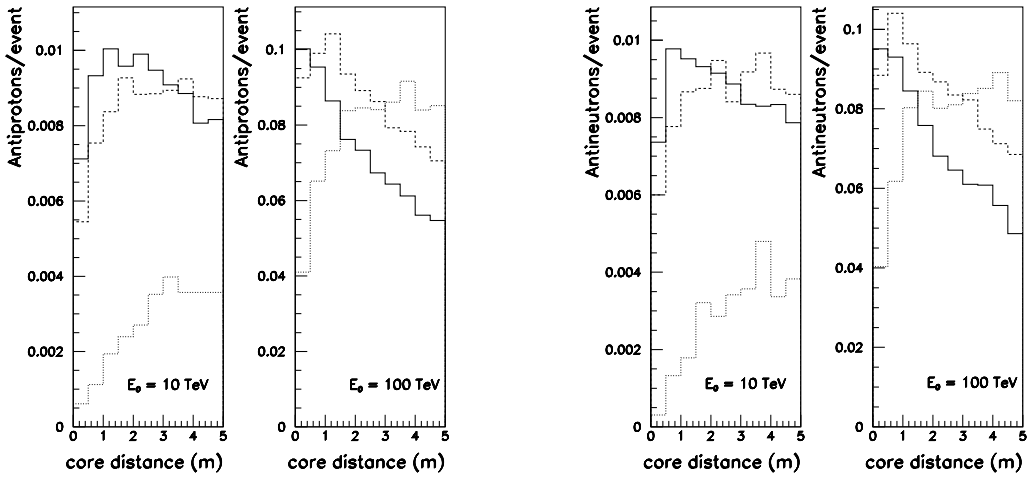

(a) (b)

Fig. 3. Lateral distribution at an atmospheric depth X= 200 g/cm^2 of (a) antiprotons and (b) antineutrons with kinetic energies $E_{kin} \geq 1$ GeV produced by vertical primary iron (solid line), α-particle (dashed line) and proton (dotted line) with fixed energies.